Integral rate constant measurements of the reaction $H+D_2 \rightarrow HD(v'=1, j')+D$ at high collision energies

D.E. Adelman, H. Xu and R.N. Zare
Department of Chemistry, Stanford University, Stanford, CA 94305, USA

Received 8 December 1992

The reaction $H+D_2 \rightarrow HD(v'=1, j')+D$ was studied using two different experimental geometries: (1) a probe-laser-induced reaction geometry and (2) an independent-photolysis laser geometry. High-energy H atoms were generated by photolysis of HI which resulted in center-of-mass collision energies of 2.2 and 2.5 eV for geometries 1 and 2, respectively. The HD product was detected using (2+1) REMPI and time-of-flight mass spectrometry. The $HD(v'=1, j')$ rotational distributions are presented; at this time no corresponding theoretical calculations are available for comparison.

1. Introduction

Comparison of rigorous quantum mechanical (QM) calculations with results of well-controlled experiments has become a reality for the $H+H_2$ reaction family since the rapid development of experimental and theoretical techniques during the 1980s. Numerous comparisons between experiment and theory have appeared in the literature over this period [1–17]. Quantitative agreement has been found between experiment and theory for integral cross section measurements for ground-state reagents up to moderate total energies (i.e. less than 1.6 eV) [1,7,11–13,17,18]. Small differences, however, appear to be present for integral cross section measurements at higher collision energies [15,17] and for reactions that involve vibrationally excited reagents [14–17,19]; in addition, small discrepancies remain between theory and experiment for differential cross section measurements [7,9,10].

Recent theoretical developments by Neuhauser et al. [17] permit comparisons in which fully converged, three-dimensional quantum scattering calculations performed on a chemically accurate ab initio potential energy surface (PES) fully simulate the experimental conditions. New calculations of the H_3 PES have demonstrated the high accuracy of the fitted surfaces used for these calculations [19,20]. Similarly, numerous experimental checks have been carried out [14,15]. The overall success of QM calculations has been remarkable, but persistent small discrepancies between theory and experiment suggest the need for further refinement of the theoretical calculations.

A possible resolution of the discrepancies for integral cross section measurements has recently been reported by Kuppermann and co-workers [21–23]. In the most recent Letter by Wu and Kuppermann [23] they demonstrate that nonadiabatic effects alter the differential and, perhaps much more surprisingly, the integral cross sections of the reaction $H+H_2 \rightarrow H_2(v', j')+H$ at $E_{rel} \approx 1.4$ eV. These nonadiabatic effects are caused by a Jahn–Teller effect [24,25] brought about by the presence of the conical intersection of the ground and first excited electronic states at ≈ 2.7 eV above the saddle point of the ground-state H_3 PES. The Jahn–Teller effect occurs for systems with doubly degenerate electronic and vibrational states, which lead to a coupling of the electronic and nuclear motions. As a result, a good approximation of the vibronic wavefunction for the system has the form [25]

$$\psi = \psi_g(q, Q)\chi^g_{vib}(Q) + \psi_{ex}(q, Q)\chi^{ex}_{vib}(Q) , \qquad (1)$$

where q and Q denote the electronic and nuclear coordinates, respectively, ψ_g and ψ_{ex} are the ground and excited state electronic wavefunctions, respectively,

that depend on q and parametrically on Q; and χ^{s}_{vib} and χ^{ex}_{vib} are the corresponding vibrational functions that depend on Q only. We emphasize that this effect is not limited to systems that are comprised of indistinguishable nuclei [26].

An interesting property of the electronic wavefunctions (taken to be real) is that they change sign when transported adiabatically around a loop that encloses the conical intersection; the vibrational factors also change sign such that ψ is single valued. This phenomenon is a special case of the geometric Berry phase [24,27]. The change in sign of the electronic wavefunction can be understood in terms of an argument first presented by Longuet-Higgins [26]. The path around the conical intersection consists of a series of permutations of the relative positions of the nuclei, such that when any two nuclei are close together their electrons are paired. A cycle around the conical intersection for the $H+D_2$ reaction is pictorially presented in fig. 1. This diagram provides a qualitative picture of why the sign of the electronic wavefunction changes; this sign change results from the inversion of the electron spins of the D atoms during the recombination process of electrons as the atoms re-associate along the path circling the conical intersection.

Because of this sign change, scattering events in which the nuclear configuration circles the conical intersection can interfere with those that are direct; this phenomenon may be regarded as a special type of a dynamical resonance. The changes in the differential and integral cross sections of the reaction predicted by Kuppermann and co-workers are caused by the interference of the indirect and direct trajectories. This interference is limited to high energies because the indirect trajectories become significant only at high energies for which bent configurations of HD_2 are accessible (see fig. 1).

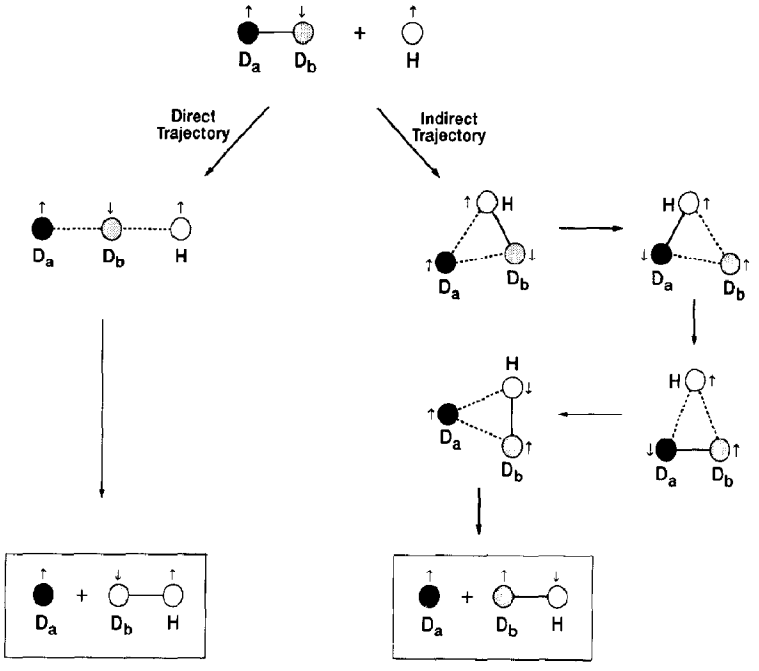

Fig. 1. Diagram of the direct and indirect trajectories for the $H+D_2$ reaction. The arrows associated with each atom designate the spin of the associated electron. Solid and dashed lines connect atoms that have strong and weak electron spin coupling between them, respectively. The change in sign of the electronic wavefunction of the system derives from the inversion of the electron spins on the D_a and D_b atoms. The permutation of the coupling of electron spins between the three atoms causes this spin inversion. The electron spin of a strongly coupled atom is preserved over that of a weakly coupled atom for each permutation. The spin of the "free" H atom is arbitrarily chosen to be "spin up".

The purpose of the present Letter is to present results of additional experiments at higher total energies than previously reported and under well controlled conditions. These experiments provide new data that can be used to determine the importance of the Jahn–Teller effect in this reactive scattering system. Also, we expect that at the high energies accessed by these experiments, new theoretical techniques will need to be developed in which both the ground and first excited electronic surfaces are included in the dynamical calculations, in contrast to the use of a single PES in which modified boundary conditions are included to account for the presence of the other PES [28]. We have carried out these experiments with these future developments in mind.

2. Experimental

The experimental setups for the probe-laser-induced and independent-photolysis geometries have been described previously [5,15]. We will provide a basic overview of the experiment. HI was purified by a freeze–pump–thaw cycle and mixed with D_2 and He in the ratio HI:D_2:He = 1:3:30. The reagent mix flowed into a high-vacuum chamber via a pulsed, supersonic nozzle. The measured rotational temperature of D_2 was 150 K for these experiments, and the collision energy spread [29] was 0.096 and 0.098 eV for the 2.2 and 2.5 eV experiments, respectively. For the 2.2 eV experiment the probe laser pulse initiated the reaction by photolysis of HI and state-specifically ionized the HD reaction product via (2+1) resonance-enhanced multiphoton ionization. Because the same laser pulse initiated the reaction and detected the HD product, the observed reaction products were formed within the ≈5 ns pulse duraction. For the 2.5 eV experiment the independent-photolysis beam was focused into the chamber by a quartz lens (210 mm f.l.) mounted on an x–y–z translation stage, which allowed optimization of the overlap with the counterpropagating probe beam. The HD^+ ions were detected in a shuttered time-of-flight mass spectrometer. This detection scheme has been calibrated against a high-temperature, effusive nozzle [30,31].

As in previous independent-photolysis studies, an every-other-shot subtraction procedure was used to remove the probe-laser contribution to the ion signal. This procedure involved varying the delay between the photolysis and probe lasers between ≈11 and ≈55 ns on alternate pulses. At each delay the probe-laser-induced signal was the same while the photolysis-laser-induced reaction signal increased because of product buildup. This procedure results in signal exclusively from the photolysis-laser-induced reaction.

The probe laser consisted of a 10 Hz, Nd:YAG-pumped dye laser (Spectra Physics, DCR-3G, PDL-1) with frequency-doubling and mixing stages (INRAD Autotracker II, β-barium borate (BBO) crystals[#1]). A 10 Hz Nd:YAG-pumped dye laser (Spectra Physics, GCR-4, PDL-1) with frequency-doubling and mixing stages generated the 202 nm photolysis beam for the 2.5 eV experiment.

UV laser photolysis of HI was used to generate translationally hot H atoms. Photolysis of HI produces two groups of H atoms with different speeds, which correspond to the production of I and I*. For the independent-photolysis experiment the I*/I ratio was 0.15 [32] where E_{rel} was 2.5 and 1.7 eV for the fast and slow H-atom channels, respectively.

When HI was photolyzed by the tunable probe laser (λ=209–218 nm), the photolysis wavelength and therefore E_{rel} varied as different HD($v'=1, j'$) levels were detected. E_{rel} varied from 2.3 and 1.6 eV for the fast and slow channels, respectively, at HD($v'=1$, $j'=0$) to 2.1 and 1.4 eV for the fast and slow channels, respectively, at HD($v'=1, j'=15$). The I*/I ratio varied with probe-laser wavelength and ranged from 0.36 at HD($v'=1, j'=0$) to 0.97 at HD($v'=1$, $j'=15$) [32].

The H+DI(D+HI) reactions introduced no interference because of the low isotopic abundance of D atoms; in addition, we used a very dilute mix of HI. Product fly-out for the independent-photolysis experiment was tested by carrying out the experiment at a shorter photolysis/probe laser time delay (30 ns instead of 55 ns). No evidence of product fly-out was found. The HD($v'=1, j'$) rotational distributions were each recorded 11 times at E_{rel}=2.2 and

[#1] The BBO crystals were supplied by R.S. Feigelson and R.K. Route and grown as part of a research program sponsored in part by the Army Research Office, Contract No. DAAL03-86-K-0129, and in part by the NSF/MRL Program through the Center for Materials Research, Stanford University.

2.5 eV over 3 and 4 separate days, respectively.

3. Results and discussion

Rotational product state distributions were measured for the reaction $H+D_2 \rightarrow HD(v'=1, j')+D$ at $E_{rel}=2.2$ and 2.5 eV. The rotational distributions at $E_{rel}=2.2$ and 2.5 eV are presented in figs. 2 and 3,

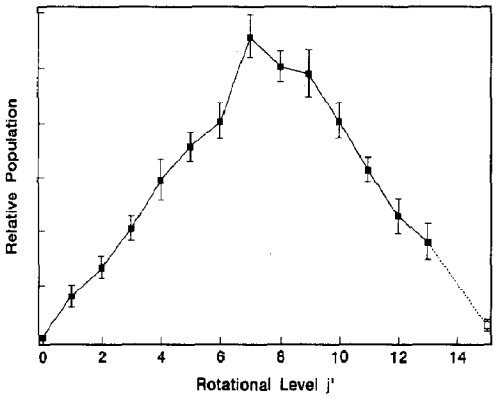

Fig. 2. Rotational distributions of the $H+D_2 \rightarrow HD(v'=1, j')+D$ at $E_{rel} \approx 2.2$ eV using a probe-laser-induced reaction geometry. Error bars represent one standard deviation. Dotted lines connect the populations of levels adjacent to a level for which the population was not measured. Closed markers denote calibrated levels and the open marker denotes an uncalibrated level.

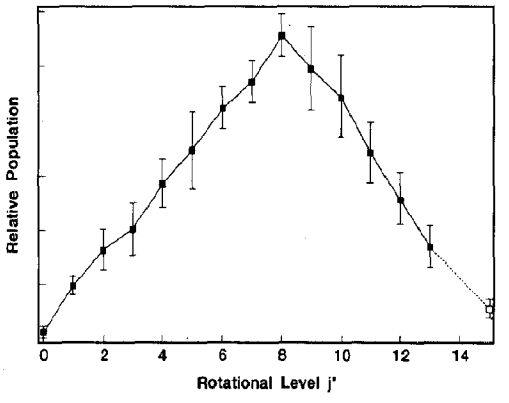

Fig. 3. Rotational distributions of the $H+D_2 \rightarrow HD(v'=1, j')+D$ at $E_{rel}=2.5$ eV using an independent-photolysis geometry. Error bars represent one standard deviation. Dotted lines connect the populations of levels adjacent to a level for which the population was not measured. Closed markers denote calibrated levels and the open marker denotes an uncalibrated level.

Table 1
Rotational product state distributions for the $H+D_2 \rightarrow HD(v'=1, j')+D$ at $E_{rel}=2.2$ and 2.5 eV

j'	E_{rel} (eV)	
	2.2	2.5
0	0.01±0.001	0.008±0.002
1	0.025±0.004	0.026±0.004
2	0.036±0.004	0.04±0.008
3	0.051±0.005	0.05±0.01
4	0.07±0.008	0.066±0.009
5	0.083±0.006	0.079±0.015
6	0.093±0.007	0.096±0.008
7	0.125±0.008	0.106±0.008
8	0.114±0.006	0.124±0.008
9	0.111±0.009	0.111±0.016
10	0.093±0.008	0.1±0.016
11	0.074±0.005	0.078±0.012
12	0.056±0.007	0.06±0.01
13	0.046±0.007	0.041±0.008
14	a)	a)
15	0.014±0.002	0.017±0.004

a) Not recorded because of a spectral overlap with a transition that originated in $HD(v'=2, j'=1)$.

respectively, and listed in table 1. The distributions are both smoothly varying and unimodal. There is a one-quantum shift in the peak of the $HD(v'=1, j')$ rotational distribution between the 2.2 and 2.5 eV experiments. Overall, however, the distributions are very similar; this consistency is expected because the total energies of the two distributions differ only by about 15%.

The present work supersedes the study by Rinnen et al. [5] for the reaction $H+D_2 \rightarrow HD(v'=1, j')+D$ at $E_{rel}=2.2$ eV. The relative collision energy spread of the present results is a factor of 5 less than that for the earlier work. Nevertheless, the agreement between the two $HD(v'=1, j')$ distributions is very good. The previous work also includes measurements of the rotational product state distributions for $v'=0$ and 2 and the vibrational product state distribution for the $H+D_2$ reaction at $E_{rel}=2.2$ eV.

These experiments represent the highest total energy and highest relative collision energy measurements of internal state distributions of the hydrogen-atom hydrogen-molecule exchange reaction. As such, it is hoped that these internal state distributions will serve as useful tests of future theoretical calculations.

Acknowledgement

We thank N.E. Shafer for many useful discussions and for experimental assistance. DEA gratefully acknowledges the Natural Sciences and Engineering Research Council (Canada) for a postgraduate scholarship. This project is supported by the National Science Foundation under Grant No. NSF CHE-89-21198.

References

[1] D.P. Gerrity and J.J. Valentini, J. Chem. Phys. 81 (1984) 1298.
[2] R.S. Blake, K.-D. Rinnen, D.A.V. Kliner and R.N. Zare, Chem. Phys. Letters 153 (1988) 365.
[3] J.Z.H. Zhang and W.H. Miller, Chem. Phys. Letters 153 (1988) 465.
[4] J.-C. Nieh and J.J. Valentini, Phys. Rev. Letters 60 (1988) 519.
[5] K.-D. Rinnen, D.A.V. Kliner, R.S. Blake and R.N. Zare, Chem. Phys. Letters 153 (1988) 371.
[6] J.M. Launay and M.L. Dourneuf, Chem. Phys. Letters 163 (1989) 178.
[7] J.Z.H. Zhang and W.H. Miller, J. Chem. Phys. 91 (1989) 1528.
[8] D.A.V. Kliner, K.-D. Rinnen and R.N. Zare, Chem. Phys. Letters 166 (1990) 107.
[9] S.A. Buntin, C.F. Giese and W.R. Gentry, Chem. Phys. Letters 168 (1990) 513.
[10] R.E. Continetti, B.A. Balko and Y.T. Lee, J. Chem. Phys. 93 (1990) 5719.
[11] M. Zhao, D.G. Truhlar, D.W. Schwenke and D.J. Kouri, J. Phys. Chem. 94 (1990) 7074.
[12] M. D'Mello, D.E. Manolopoulos and R.E. Wyatt, J. Chem. Phys. 94 (1991) 5985.
[13] D.A.V. Kliner, D.E. Adelman and R.N. Zare, J. Chem. Phys. 94 (1991) 1069.
[14] D.A.V. Kliner, D.E. Adelman and R.N. Zare, J. Chem. Phys. 95 (1991) 1648.
[15] D.E. Adelman, N.E. Shafer, D.A.V. Kliner and R.N. Zare, J. Chem. Phys. 97 (1991) 7323.
[16] S.L. Mielke, R.S. Friedman, D.G. Truhlar and D.W. Schwenke, Chem. Phys. Letters 188 (1992) 359.
[17] D. Neuhauser, R.S. Judson, D.J. Kouri, D.E. Adelman, N.E. Shafer, D.A.V. Kliner and R.N. Zare, Science 257 (1992) 519.
[18] D.A.V. Kliner, K.-D. Rinnen and R.N. Zare, J. Chem. Phys. 90 (1989) 4625.
[19] W.J. Keogh, A.I. Boothroyd, P. Martin, S.L. Mielke, D.G. Truhlar and D.W. Schwenke, Chem. Phys. Letters 195 (1992) 144.
[20] D.L. Diedrich and J.B. Anderson, Science 258 (1992) 786.
[21] B. Lepetit and A. Kuppermann, Chem. Phys. Letters 166 (1990) 581.
[22] Y.-S.M. Wu, A. Kuppermann and B. Lepetit, Chem. Phys. Letters 186 (1991) 319.
[23] Y.-S.M. Wu and A. Kuppermann, Chem. Phys. Letters 201 (1993) 178.
[24] H.C. Longuet-Higgins, in: Molecular spectroscopy; methods and applications in chemistry, eds. G.H. Beaven and E.A. Johnson (Macmillan, New York, 1961) p. 446.
[25] G. Herzberg, Molecular spectra and molecular structure, Vol. 3. Electronic spectra and electronic structure of polyatomic molecules (Van Nostrand Reinhold, New York, 1966).
[26] H.C. Longuet-Higgins, Proc. Roy. Soc. A 344 (1975) 147.
[27] C.A. Mead and D.G. Truhlar, J. Chem. Phys. 70 (1979) 2284.
[28] B. Lepetit, Z. Peng and A. Kuppermann, Chem. Phys. Letters 166 (1990) 572.
[29] W.J. van der Zande, R. Zhang and R.N. Zare, in: Spectral line shapes, Vol. 6, eds. L. Frommhold and J.W. Keto (American Institute of Physics, New York, 1990) p. 301; W.J. van der Zande, R. Zhang, R.N. Zare, K.G. McKendrick and J.J. Valentini, J. Phys. Chem. 95 (1991) 8205.
[30] K.-D. Rinnen, M.A. Buntine, D.A.V. Kliner, R.N. Zare and W.M. Huo, J. Chem. Phys. 95 (1991) 214.
[31] W.M. Huo, K.-D. Rinnen and R.N. Zare, J. Chem. Phys. 95 (1991) 205.
[32] I. Levy and M. Shapiro, J. Chem. Phys. 89 (1988) 2900.